

# AdaIAT: Adaptively Increasing Attention to Generated Text to Alleviate Hallucinations in LVLM

Li'an Zhong<sup>1</sup>, Ziqiang He<sup>1</sup>, Jibin Zheng<sup>2</sup>, Jin Li<sup>1</sup>, Z. Jane Wang<sup>3</sup>, Xiangui Kang<sup>1\*</sup>  
<sup>1</sup>Sun Yat-Sen University, <sup>2</sup>Foshan University, <sup>3</sup>University of British Columbia

## Abstract

Hallucination has been a significant impediment to the development and application of current Large Vision-Language Models (LVLMs). To mitigate hallucinations, one intuitive and effective way is to directly increase attention weights to image tokens during inference. Although this effectively reduces the hallucination rate, it often induces repetitive descriptions. To address this, we first conduct an analysis of attention patterns and reveal that real object tokens tend to assign higher attention to the generated text than hallucinated ones. This inspires us to leverage the generated text, which contains instruction-related visual information and contextual knowledge, to alleviate hallucinations while maintaining linguistic coherence. We therefore propose *Increase Attention to Generated Text (IAT)* and demonstrate that it significantly reduces the hallucination rate while avoiding repetitive descriptions. To prevent naive amplification from impairing the inherent prediction capabilities of LVLMs, we further explore *Adaptive IAT (AdaIAT)* that employs a layer-wise threshold to control intervention time and fine-grained amplification magnitude tailored to the characteristics of each attention head. Both analysis and experiments demonstrate the effectiveness of AdaIAT. Results of several LVLMs show that AdaIAT effectively alleviates hallucination (reducing hallucination rates  $C_S$  and  $C_I$  on LLaVA-1.5 by 35.8% and 37.1%, respectively) while preserving linguistic performance and prediction capability, achieving an attractive trade-off. Code is available at <https://github.com/XianguiKang/AdaIAT.git>.

## 1. Introduction

Large Vision-Language Models (LVLMs) [3, 8, 38] integrate pre-trained visual encoders with Large Language Models (LLMs) to achieve cross-modal alignment and joint representation learning, enabling applications encompassing cross-modal content generation, image captioning, embodied intelligence interaction, and similar scenarios. How-

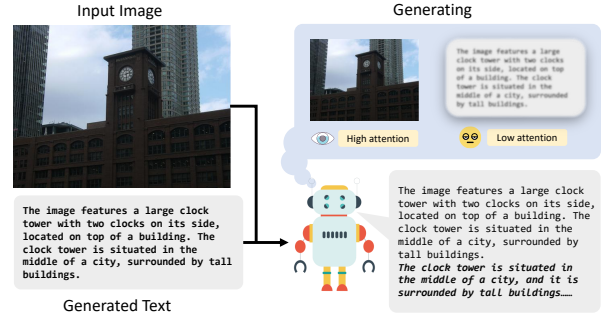


Figure 1. Case illustration: The attention intervention methods amplify the attention to image tokens, thereby emphasizing visual information and mitigating hallucinations. However, the relatively low attention to the generated text causes the model to forget preceding utterances, leading to repetitive descriptions of the prominent object ‘clock tower’.

ever, current LVLMs all face the significant challenge of hallucinations, manifested as generating descriptions inconsistent with the input visual content, which severely constrains their reliability and practical utility.

Recent studies indicate that hallucinations arise from insufficient alignment between visual and linguistic features during the cross-modal fusion process, leading LVLMs to “ignore” the image content [5, 14, 27, 29]. Therefore attention intervention methods (such as PAI[21], HGAI[14]) were proposed to directly amplify the attention weights assigned to image tokens during the generation process, thereby emphasizing the importance of visual information and reducing the hallucination rate. Although such methods are intuitive and attractive, we observed that the reduced hallucination rates achieved by these methods often come at the cost of degraded linguistic capability.

Fig. 1 illustrates a case of degradation in linguistic capability: PAI excessively enhances attention to the image, relatively suppressing attention to the text. This leads LVLMs to “forget” previously generated content, sometimes even producing output nearly identical to the preceding sentence. While such attention intervention suppresses hallucinations, it sacrifices the core linguistic capability of the LLM, deviating from the user’s original intent. To address this issue, we first analyze the attention patterns of real versus halluci-

\*Corresponding author.

nated object sets and note that, compared to hallucinated objects, real objects exhibit higher attention to generated text tokens ( $T_p$ ). This insight suggests that the knowledge contained in  $T_p$  may support accurate predictions. Intuitively, this makes sense: due to the causal attention mechanism during generation,  $T_p$ , as the output of the LVLM, naturally contains instruction-related visual information. As prior research [14, 21] has shown that amplifying attention to visual information can mitigate hallucinations, would increasing attention to  $T_p$  be similarly effective?

Motivated by the above observation, we propose *Increased Attention to Generated Text* (IAT) to leverage instruction-related visual information and contextual knowledge embedded in  $T_p$ : the former supports more accurate image descriptions, while the latter maintains linguistic coherence and diversity. Experimental results demonstrate that IAT effectively suppresses hallucinations without introducing repetitive descriptions. Furthermore, we notice that existing attention amplification methods typically intervene throughout the entire process regardless of whether a hallucination is present, and apply a uniform amplification magnitude that overlooks the distinct roles of different attention heads. Such coarse and unnatural intervention may disrupt the model’s inherent reasoning process. To address this, we further propose *Adaptive IAT* (AdaIAT), which incorporates layer-wise thresholds to control the intervention timing and adaptively assigns distinct amplification magnitudes to different attention heads.

In summary, the contributions of this paper are three-fold: 1) We propose IAT, which increases attention to generated text tokens to leverage the model’s prior compressed, instruction-relevant visual representations, thereby effectively reducing hallucinations and avoiding repetitive description. 2) We further propose AdaIAT to adaptively determine both the intervention timing and amplification magnitudes, which minimizes the disruption to the inherent prediction patterns of the underlying LLM. 3) Both analysis and experiments demonstrate the effectiveness of the proposed AdaIAT. Compared with current attention intervention methods on different LVLMs, our AdaIAT significantly reduces hallucination rates while maintaining prediction capability and textual diversity.

## 2. Related Work

### 2.1. Large Vision-Language Models

Advances in pre-training [7] and instruction fine-tuning [30] techniques have propelled the development of large language models (LLMs) such as LLaMA [28] and Vicuna [22], which have promoted the rise of large visual language models (LVLMs). Pioneering works such as Flamingo [1] and BLIP-2 [18] successfully adapted LLMs to visual tasks, demonstrating generative and con-

textual learning capabilities. Recently, visual instruction fine-tuning has further improved the capabilities of LVLMs, which usually includes a visual encoder (such as CLIP [23]), a modality connector (aligning image features to the text domain), and LLMs. LLaVA-1.5 [20] utilizes an MLP as its linear projection layer and incorporates an AnyRes strategy to accommodate input images of varying sizes. Janus-Pro [9] decouples multimodal understanding and generation via separate visual encoders and task-specific adapters, projecting their outputs into a unified sequence processed by LLM. Qwen2.5-VL [4] introduces dynamic resolution processing and absolute time encoding to accommodate complex inputs, and further integrates window attention into its vision encoder to reduce computational overhead. Despite their remarkable capabilities, existing LVLMs generally suffer from the serious problem of hallucination, which has become an increasingly prominent research focus in recent years.

### 2.2. Hallucination and Its Mitigation in LVLMs

Hallucination in LVLMs specifically refers to the phenomenon where the text descriptions generated by LVLMs contradict the content of the input images, such as describing objects that do not exist in the image, which severely compromises model reliability. To mitigate this issue, researchers [26, 31, 40] have proposed multiple technical approaches: (1) Introducing additional datasets for training: compensating for data bias and cross-modal knowledge gaps by incorporating higher-quality annotated data [12], or enhancing vision-language alignment training [25]. (2) Post-hoc correction: LURE [37] trains an LVLMs as a revisor to rewrite sentences, while Woodpecker [32] extracts key concepts for subsequent verification and correction using expert models. (3) Decoding strategies [10, 35]: VCD [16] mitigates over-reliance on statistical biases and language priors by contrasting output distributions generated from original versus distorted visual inputs, whereas AGLA [2] decodes the outputs using an assembly of global and local attention. (4) Attention intervention: PAI [21] globally enhances the attention on image tokens to emphasize visual information importance, while HGAI [14] amplifies the attention to image tokens by integrating information from multiple attention heads. Unlike prior methods that often introduce substantial computational overhead during training or inference, attention intervention significantly reduces hallucination rates while maintaining lower inference costs, achieving the best performance in hallucination mitigation. However, they may exhibit compromised language capabilities in some cases.

## 3. Methodology

The input to LVLMs comprises both text and images. LVLMs project contents from different modalities into to-

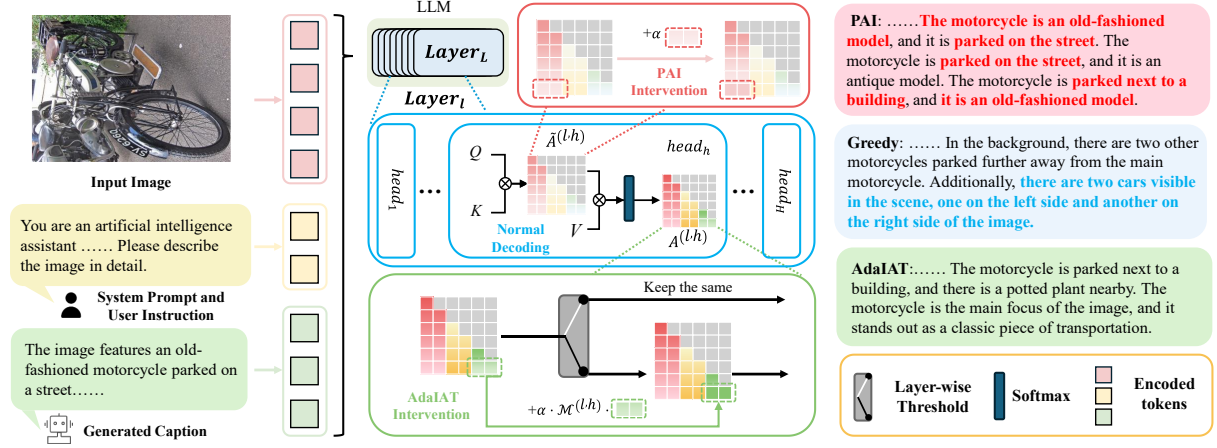


Figure 2. The mechanisms of mitigating hallucination based on Greedy in PAI and AdaIAT, with repeated descriptions annotated in **red** and hallucinations annotated in **blue**. While Greedy generates the hallucinated object “cars”, PAI enhances attention to image tokens with a fixed  $\alpha$  to mitigate hallucination. However, it suffers from repeated subjects and monotonous, redundant language. In contrast, AdaIAT employs layer-wise thresholds to control the amplification and designs  $\mathcal{M}^{(l,h)}$  for each attention head to adaptively enhance attention towards the generated text tokens, which produces accurate and hallucination-free captions.

kens within a unified input feature space  $I_s$  using corresponding domain-specific encoders. These tokens are then fed into the pre-trained LLM. As shown in Fig. 2, at timestep  $n$ , to predict the next text token  $t_{n+1}$ , the LLM’s input  $\mathcal{I}$  consists of: system prompt tokens  $S = \{s_1, \dots, s_a\}$ , image features tokens  $V = \{v_1, \dots, v_m\}$ , user instruction tokens  $U = \{u_1, \dots, u_b\}$ , and generated text tokens  $T_p = \{t_1, \dots, t_n\}$ . The total input length is  $len = a + m + b + n$ . Typically, the LLM incorporates  $L$  layers of attention blocks, with each layer containing  $H$  attention heads. For the  $h$ -th head in the  $l$ -th layer, we focus on the self-attention computation pertaining to the token  $t_n$  as follows:

$$\mathbf{A}^{(l,h)} = \text{softmax}(\tilde{\mathbf{A}}^{(l,h)}) \quad (1)$$

$$\tilde{\mathbf{A}}^{(l,h)} = \frac{\mathbf{Q}_{t_n}^{(l,h)} (\mathbf{K}^{(l,h)})^\top}{\sqrt{d_k}} \quad (2)$$

Here,  $l \in (1, L)$ ,  $h \in (1, H)$ ,  $\mathbf{Q}_{t_n}^{(l,h)}$  denotes the query vector corresponding to  $t_n$ , and  $\mathbf{K}^{(l,h)}$  denotes the key vectors for all tokens. During the prediction process of  $t_{n+1}$ , we can obtain the attention maps  $\mathbf{A} \in \mathbb{R}^{L \times H \times len}$  from all layers and heads. Let  $\mathbf{A}^{(l,h)}(i)$  denote the attention weight to the  $i$ -th token during prediction, where  $i \in (1, len)$ .

### 3.1. Observation and Analysis

To investigate the causes of hallucination, we analyzed the differences in internal patterns during the generation of real versus hallucinated objects. Specifically, we randomly selected 10,000 images from COCO 2014 [19] and generated captions for them using LLaVA-1.5-7B, with the prompt:

“Please describe the image in detail.” (Results of other LVLMs are provided in the Appendix.) By identifying objects in the captions through ground truth annotations, we obtained 22,015 real objects tokens and 9,473 hallucinated objects tokens. We collected their corresponding attention weight maps subsets  $D^r$  and  $D^h$ , and computed their average attention maps  $\mathbf{A}^r, \mathbf{A}^h \in \mathbb{R}^{L \times H \times len}$ . To quantify the importance of different inputs to model outputs, we aggregate attention across specific regions, for example, for  $T_p$ :

$$\mathbf{A}_{T_p}^{(l,h)} \triangleq \frac{1}{n} \sum_i \mathbf{A}^{(l,h)}(i), \quad \mathcal{I}(i) \in T_p \quad (3)$$

Then we obtain  $\mathbf{A}_{T_p} \in \mathbb{R}^{L \times H}$ , representing the average per-token attention weights from  $t_{n+1}$  to  $T_p$  across different layers and attention heads. Further, we aggregate attention across the heads:

$$\bar{\mathbf{A}}_{T_p}^{(l)} \triangleq \sum_{h=1}^H \mathbf{A}_{T_p}^{(l,h)} \quad (4)$$

We use  $(\bar{\cdot})$  to denote the average of the heads, then we obtain  $\bar{\mathbf{A}}_{T_p} \in \mathbb{R}^L$ , indicating the importance of  $T_p$  across different layers. Then, we correspondingly compute  $\bar{\mathbf{A}}_V, \bar{\mathbf{A}}_V^r$  for input image. Subsequently, we compute  $\bar{\mathbf{A}}_{T_p}^r, \bar{\mathbf{A}}_{T_p}^h, \bar{\mathbf{A}}_V^r$ , and  $\bar{\mathbf{A}}_V^h$  from  $D^r$  and  $D^h$ , and visualize them in Figure 3.

Consistent with existing research [14], hallucination correlates with insufficient attention to  $V$ , manifested as  $\bar{\mathbf{A}}_V^r$  consistently exceeds  $\bar{\mathbf{A}}_V^h$  (typically by a factor of  $\times 1$ – $\times 1.5$ ) in Fig. 3b. However, we observe an intriguing phenomenon: as depicted in Fig. 3a, **the discrepancy between real and hallucinated objects is more pronounced in  $\bar{\mathbf{A}}_{T_p}^r$  and  $\bar{\mathbf{A}}_{T_p}^h$  (typically by a factor of  $\times 1.5$ – $\times 2.5$ ), indicating that real ob-**

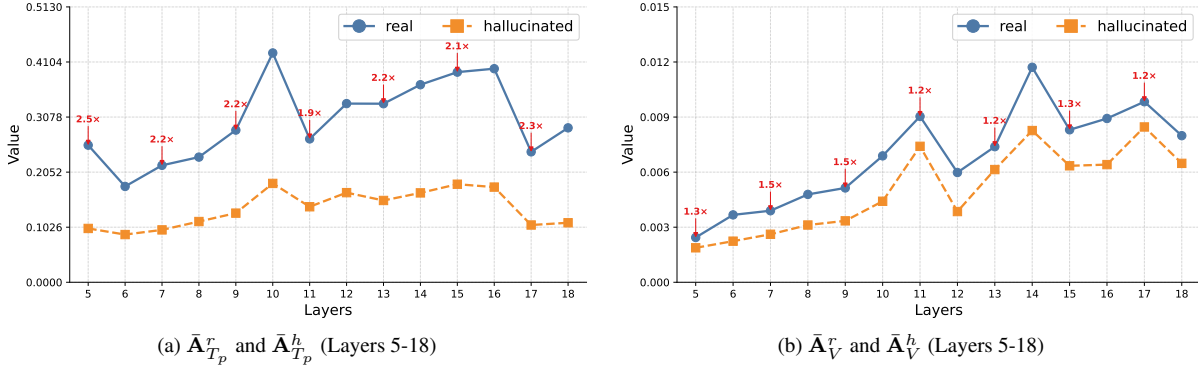


Figure 3. Visualization of the average per-token attention weights from text token  $t_{n+1}$  to generated text tokens  $T_p$  ( $\bar{A}_{T_p}^r$  and  $\bar{A}_{T_p}^h$ ) and to image tokens  $V$  ( $\bar{A}_V^r$  and  $\bar{A}_V^h$ ), showing only layers 5–18 for clearer observation.

**ject tokens exhibit stronger attention to  $T_p$ .** This suggests that knowledge from  $T_p$  may support accurate predictions.

To explain this phenomenon, we re-examine the nature of  $V$  and  $T_p$ . It is noteworthy that  $V$ , encoded by the visual encoder, is heterogeneous to the LLM. Even after fine-tuning efforts to align  $V$  with  $I_s$ , an inevitable domain gap persists between them. This gap is widely recognized in many studies [13, 33] as a significant cause of hallucinations. Furthermore,  $V$  focuses solely on encoding visual information and is independent of text, thus containing a large amount of instruction-irrelevant visual information. However, during generation, the LLM has access to both the image and user instructions, enabling it to purposefully organize and summarize instruction-related visual information to successfully generate  $T_p$ . Consequently,  $T_p$  inherently encodes instruction-related visual information and naturally belongs to  $I_s$ .

Therefore, during the generation of each token in  $T_p$ , the visual content in  $V$ , which contains substantial instruction-irrelevant information and deviates from  $I_s$ , is reorganized into  $T_p$ , which is instruction-relevant and inherently belongs to  $I_s$ . This process produces concentrated and condensed visual features while mitigating the gap between visual features and the text-dominated feature space  $I_s$ , thereby reducing hallucination and supporting more accurate predictions. Given this observation, might we exploit the visual feature embedded in  $T_p$  to alleviate hallucinations?

### 3.2. Increasing Attention to $T_p$

Motivated by the above insight, we pursued further investigation. To leverage the visual information embedded within  $T_p$ , we propose Increased Attention to  $T_p$  (IAT). Specifically, for the intermediate layers of the LLM (i.e., layers 5-18), we employ a naive attention amplification mechanism to increase the attention to  $T_p$ :

$$\tilde{A}^{(l,h)}(i) = \bar{A}^{(l,h)}(i) + \alpha \cdot |\bar{A}^{(l,h)}(i)|, \quad (5)$$

where  $\alpha$  is the amplification factor,  $l \in (5, 18)$  and  $\mathcal{I}(i) \in T_p$ . In PAI,  $\mathcal{I}(i) \in V$ , which is the most critical distinction

compared to our approach.

To evaluate the effectiveness of our method, we compare it against PAI, HGAI, and the Greedy decoding. To quantify hallucination rates and linguistic richness in captions, we employ the CHAIR [24] and Distinct-1 [17] metrics. The CHAIR metric quantifies hallucination by verifying whether objects mentioned in captions actually appear in the image, comprising  $CHAIR_S$  ( $C_S$ ) and  $CHAIR_I$  ( $C_I$ ), which assess sentence-level and instance-level hallucinations respectively:

$$C_S = \frac{|\{\text{captions with hallucinated objects}\}|}{|\{\text{all captions}\}|} \quad (6)$$

$$C_I = \frac{|\{\text{hallucinated objects}\}|}{|\{\text{all mentioned objects}\}|} \quad (7)$$

Distinct-n is a widely used metric for textual diversity assessment, measuring diversity by calculating the proportion of unique n-grams in the generated text:

$$\text{Distinct} - n = \frac{\text{unique ngram}}{\text{total ngram}} \quad (8)$$

Specifically, Distinct-1 ( $D_1$ ) evaluates lexical richness and the ability to avoid repetitive patterns in generated text. A higher  $D_1$  score indicates richer vocabulary usage and fewer repetitive descriptions.

We randomly selected 500 images from COCO [19] and generated captions for them using the above four methods on LLaVA-1.5-7B, with the prompt ‘‘Please describe the image in detail.’’ For the attention intervention methods, a larger  $\alpha$  in Eq. 5 represents a stronger intervention on the model. While this achieves a lower hallucination rate, it inevitably causes greater impairment to certain aspects of the model (e.g, text diversity). Therefore, for PAI, HGAI, and IAT, we varied  $\alpha$  and plotted their performance trade-offs between  $C_s$  and  $D_1$  in Fig. 4, with the  $D_1$  of the Greedy decoding annotated for reference. It demonstrates that increasing attention to  $T_p$  effectively mitigates hallucination, providing preliminary validation of our motivation. Additionally, as the hallucination rate decreases, both PAI and HGAI exhibit a noticeable decline in text diversity.

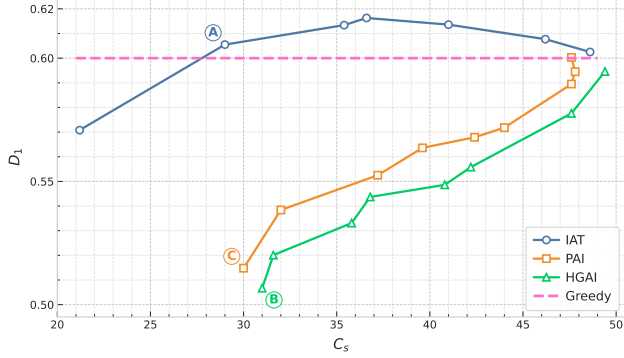


Figure 4. Trends of textual diversity  $D_1$  for different methods as the hallucination rate  $C_S$  decreases. The dashed line denotes the  $D_1$  of the original greedy decoding as a reference. Regions closer to the top-left indicate better performance.

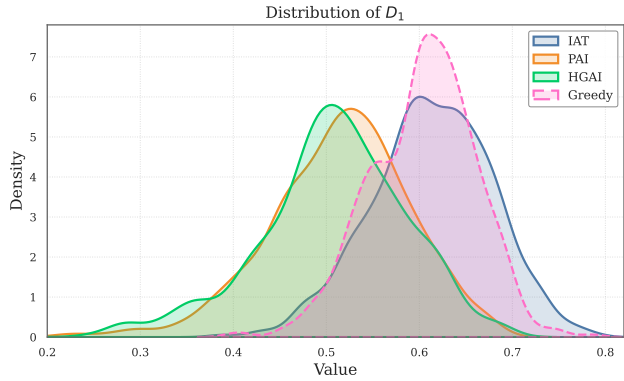


Figure 5. The distributions of textual diversity  $D_1$  for captions generated by different methods using the LLaVA-1.5-7B, where a higher  $D_1$  corresponds to greater text diversity. The distribution is partially truncated for better visualization.

We further selected Greedy and three points (A, B, C) with approximate hallucination rates from Fig. 4 and calculated the  $D_1$  distributions for their captions and show it in Fig. 5. We observe that compared to Greedy, PAI and HGAI show a pronounced shift towards lower values, indicating more repetitive descriptions in captions. In contrast, IAT maintains a distribution comparable to Greedy, even exhibiting a higher proportion in the high-score range (0.65-0.8), which suggests that IAT can enhance the diversity of the captions. This occurs because PAI and HGAI increase attention to all image tokens, which relatively suppresses attention to  $T_p$ . Consequently, the model “forgets” previously generated content and tends to repetitively describe the salient objects in the image, leading to redundant language. In contrast, IAT avoids this by increasing attention to  $T_p$ , leveraging contextual knowledge to ensure coherent and diverse text generation.

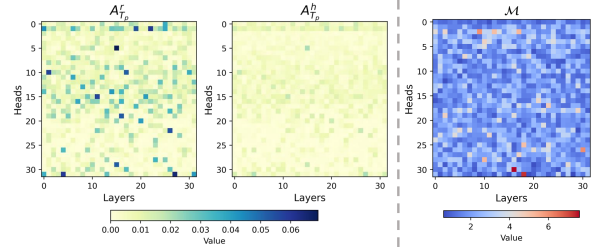


Figure 6. Characteristics of different heads on LLaVA-1.5-7B. Left: Visualization of the average per-token attention weight to generated text for each layer and head, computed over the sets of real objects ( $\mathbf{A}_{T_p}^r$ ) and hallucinated objects ( $\mathbf{A}_{T_p}^h$ ). Right: The visualization of  $\mathbf{A}_{T_p}^r/\mathbf{A}_{T_p}^h$ . Though  $\mathbf{A}_{T_p}^r$  is generally higher than  $\mathbf{A}_{T_p}^h$ , the fold-difference varies across different heads.

### 3.3. Adaptive Attention Enhancement

While the naive attention amplification method is straightforward and effective, it suffers from several limitations. Therefore, we propose **Adaptive IAT (AdaIAT)**, adaptively determining both the time to intervene and the amplification magnitude. This is achieved by monitoring attention patterns during inference and leveraging the different patterns of  $\mathbf{A}^r$  versus  $\mathbf{A}^h$  across different attention heads. AdaIAT is meticulously designed to minimize disruption to the model’s standard prediction while simultaneously maintaining potent hallucination mitigation performance.

#### 3.3.1. Adaptively Determine the Amplification Time

Naive amplification persistently boosts attention towards  $T_p$  regardless of whether hallucination tendencies arise. However, hallucinations are sporadic phenomena and LVLMs typically exhibit accurate predictions. Blindly amplifying attention indiscriminately may lead to abnormally high attention on  $T_p$  during normal predictions, impairing the model’s standard prediction capabilities and consequently affecting accuracy. An effective amplification strategy should dynamically monitor the attention patterns, promptly detect anomalies (e.g., excessively low attention towards  $T_p$ ), and then trigger IAT. Therefore, we establish a layer-wise threshold:

$$\mathcal{T} = \bar{\mathbf{A}}_{T_p}^h + \beta(\bar{\mathbf{A}}_{T_p}^r - \bar{\mathbf{A}}_{T_p}^h) \quad (9)$$

where  $\beta$  is a balanced coefficient,  $\mathcal{T} \in \mathbb{R}^L$  and  $\mathcal{T}^{(l)}$  denotes the threshold for the  $l$ -th layer. During generation, when  $\mathcal{T}^{(l)} > \bar{\mathbf{A}}_{T_p}^{(l)}$ , it is considered that attention to  $T_p$  is insufficient, which serves as the trigger for IAT. When  $\mathcal{T}^{(l)} \leq \bar{\mathbf{A}}_{T_p}^{(l)}$ , it is considered that the model maintains adequate attention to  $T_p$ . In this case, the model proceeds with its normal prediction without any intervention, thereby avoiding disruption to its standard prediction behavior.

Table 1. CHAIR hallucination evaluation of various methods on three LVLMs. The best values (excluding Greedy) are highlighted in **bold**. † indicates that the attention intervention is applied based on the Sample decoding.

Models	LLaVA-1.5-7B[20]				LLaVA-1.5-13B[20]				Janus-Pro-7B[9]				Qwen2.5-VL-7B[3]			
Metrics	$C_S \downarrow$	$C_I \downarrow$	F1 $\uparrow$	$D_1 \uparrow$	$C_S \downarrow$	$C_I \downarrow$	F1 $\uparrow$	$D_1 \uparrow$	$C_S \downarrow$	$C_I \downarrow$	F1 $\uparrow$	$D_1 \uparrow$	$C_S \downarrow$	$C_I \downarrow$	F1 $\uparrow$	$D_1 \uparrow$
Sample	53.0	15.6	73.4	0.65	52.0	13.7	74.9	0.66	34.0	9.0	73.5	0.64	42.0	11.3	72.5	0.67
AdaIAT†	42.0	12.3	73.1	0.66	37.8	10.1	75.0	0.67	29.8	8.1	72.6	0.65	34.6	9.0	75.1	0.68
Greedy	49.0	13.3	77.9	0.60	47.8	12.5	78.9	0.60	25.8	6.7	76.8	0.62	33.6	8.3	76.5	0.65
PAI[21]	31.8	7.8	77.7	0.50	34.2	9.0	<b>79.3</b>	0.56	20.4	5.6	76.1	0.61	32.0	8.2	74.7	0.64
HGAI[14]	31.4	<b>6.9</b>	78.3	0.50	26.4	7.8	76.9	0.55	21.0	5.3	75.9	0.62	30.4	8.0	<b>76.8</b>	0.65
IAT	<b>29.8</b>	9.0	76.8	<b>0.61</b>	31.0	8.6	78.6	<b>0.61</b>	20.6	5.3	75.3	<b>0.65</b>	29.2	7.7	76.4	<b>0.67</b>
AdaIAT	31.4	8.3	<b>79.4</b>	0.60	<b>25.2</b>	<b>6.1</b>	79.2	0.60	<b>19.0</b>	<b>4.9</b>	<b>76.5</b>	0.64	<b>28.4</b>	<b>6.9</b>	<b>76.8</b>	0.66

### 3.3.2. Adaptive Amplification Magnitude

In naive amplification, a fixed  $\alpha$  is uniformly applied across all heads. However, compared to real object tokens generation, significant variations exist in different heads when hallucinated object tokens are generated. We derive  $\mathbf{A}_{T_p}^r, \mathbf{A}_{T_p}^h \in \mathbb{R}^{L \times H}$  from datasets  $D_r$  and  $D_h$  respectively, which represent the average attention to  $T_p$  across heads during real/hallucinated object generation. Subsequently, we compute the attention amplification ratio matrix:

$$\mathcal{M} = \frac{\mathbf{A}_{T_p}^r}{\mathbf{A}_{T_p}^h} \quad (10)$$

where  $\mathcal{M} \in \mathbb{R}^{L \times H}$  and  $\mathcal{M}^{(l,h)}$  represents the average attention ratio toward  $T_p$  for real versus hallucinated object generation at the  $h$ -th head of the  $l$ -th layer. We visualize  $\mathbf{A}_{T_p}^r, \mathbf{A}_{T_p}^h$ , and  $\mathcal{M}$  of LLaVA-1.5-7B in Figure 6. As observed, certain heads exhibit more significant disparities in  $\mathcal{M}$ , indicating greater attention deficiency toward  $T_p$  during hallucinated object token generation. Conversely, heads with smaller differences require smaller amplification. Thus,  $\mathcal{M}$  serves as a reliable amplification direction, shifting hallucinated attention patterns toward real attention patterns. Consequently, for the  $h$ -th head in the  $l$ -th layer, we designate  $\mathcal{M}^{(l,h)}$  as its adaptive amplification magnitude and reformulate Equation (5) as follows:

$$\mathbf{A}^{(l,h)}(i) = \mathbf{A}^{(l,h)}(i) + \alpha \cdot \mathcal{M}^{(l,h)} \cdot \mathbf{A}^{(l,h)}(i), \quad \mathcal{I}(i) \in T_p \quad (11)$$

$$\mathbf{A}^{(l,h)}(k) = \frac{\mathbf{A}^{(l,h)}(k)}{\sum_k \mathbf{A}^{(l,h)}(k)}, \quad k \in (1, len) \quad (12)$$

It is worth noting that as shown in Fig. 2, the naive amplification method intervenes on  $\hat{\mathbf{A}}$ , whereas  $\mathcal{M}$  represents the ratio of  $\mathbf{A}$  for real versus hallucinated object tokens. Therefore, in Eq. 12, we amplify  $\mathbf{A}$  and normalize it to ensure  $\sum_i \mathbf{A}^{(l,h)}(i) = 1$ , and  $\alpha$  represents the strength of amplification. In this way, AdaIAT adaptively assigns a specific amplification magnitude for each head. Heads exhibiting larger disparities in  $\mathcal{M}$  receive stronger amplification to align with real attention patterns, while those with smaller

deviations maintain weaker amplification to avoid disrupting normal attention patterns.

## 4. Experiment

### 4.1. Models and Baselines

We evaluate the effectiveness and generalizability of our method on three representative LVLMs: LLaVA-1.5[20], Janus-Pro[9], and Qwen2.5-VL[3]. All models employ the 7B versions, with LLaVA-1.5 additionally employing a 13B version to investigate scale effects. The number of max tokens for all models is set to 512. Although  $\mathcal{T}$  and  $\mathcal{M}$  are derived from COCO, they were kept fixed during evaluation on all other datasets. We used the Greedy as a reference and selected two representative attention intervention methods, PAI[21] and HGAI[14], as baselines. Unless specified, all hallucination mitigation methods are implemented based on Greedy decoding.

### 4.2. CHAIR Evaluation Results

The experimental setup for the CHAIR metric follows the configuration of Section 3.1, where we use  $C_s$  and  $C_I$  to evaluate hallucination rates,  $D_1$  to assess the textual diversity, and additionally adopt the F1 score to evaluate the richness and accuracy of generated objects, measuring models' prediction capability. Table 1 presents the experimental results of different methods on selected LVLMs. We conducted a hyperparameter search to identify the optimal performance of all methods for reporting. Detailed hyperparameter selections and comparisons with additional methods are provided in the Appendix. It can be observed that for LLaVA-1.5-7B, both PAI and HGAI demonstrate significant hallucination reduction effects. However, this improvement comes at the cost of degraded textual diversity, with  $D_1$  decreasing by approximately 15%. In contrast, IAT and AdaIAT maintain the original text diversity (sustaining  $D_1$  around 0.60) of Greedy decoding while achieving comparable low hallucination rates. This advantage stems from their increased attention to  $T_p$ , thereby preventing repetitive sentences. Moreover, they effectively leverage progressively fusion, instruction-relevant visual infor-

mation at each autoregressive step, enabling more accurate predictions with fewer hallucinations. Furthermore, compared with IAT, AdaIAT adaptively determines when to activate IAT and sets fine-grained amplification magnitudes tailored to each attention head’s characteristics, minimizing disruption to the model’s native prediction patterns. Consequently, under similar hallucination rates and text diversity, AdaIAT outperforms IAT by 2.6 in F1 score, demonstrating superior prediction capability. Similar results are observed on LLaVA-13B.

On more advanced LVLMs like Janus-Pro and Qwen2.5-VL, IAT and AdaIAT exhibit higher  $D_1$  scores than PAI and HGAI, demonstrating strengthened linguistic proficiency while maintaining comparable hallucination rate. Overall, AdaIAT achieves the lowest  $C_s$  and  $C_I$  and the highest F1 on Janus-Pro and Qwen2.5-VL while maintaining  $D_1$ , demonstrating excellent mitigation efficacy across different LVLMs. We also integrate AdaIAT with Sample decoding, which effectively alleviates hallucination while maintaining or even improving F1 and  $D_1$  scores. This confirms the effectiveness of AdaIAT across different decoding strategies.

Table 2. OpenCHAIR hallucination evaluation of different methods on LLaVA-1.5-7B.

	Greedy	PAI[21]	HGAI[14]	IAT	AdaIAT
$C_o \downarrow$	0.292	0.266	0.261	0.254	0.252
$D_1 \uparrow$	0.61	0.51	0.53	0.61	0.61

### 4.3. OpenCHAIR Evaluation Results

To further validate the effectiveness of our approach, we evaluate OpenCHAIR [6], a benchmark that extends the CHAIR metric by relaxing its strong reliance on a closed vocabulary. It first parses generated captions to extract objects, then employs an LLM to judge whether each object is real, hallucinated, or uncertain, and calculates:

$$C_o = \frac{|\{\textit{hallucinated objects}\}|}{|\{\textit{hallucinated objects and real objects}\}|}, \quad (13)$$

We employ LLaVA-1.5-7B (results for other models are detailed in the Appendix) to generate captions for 2,000 images from the OpenCHAIR dataset and summarize the results in Table 2. It is observed that while PAI and HGAI successfully suppress hallucination rates, they also incur a significant degradation in  $D_1$ . In contrast, IAT and AdaIAT maintain a  $D_1$  score around 0.61 while achieving even lower hallucination rates. This further demonstrates that enhancing attention to  $T_p$  is effective in mitigating hallucination without compromising language quality.

### 4.4. GPT-4 Assisted Evaluation

To more comprehensively evaluate other kinds of hallucinations in captions, such as attributes, positions, and re-

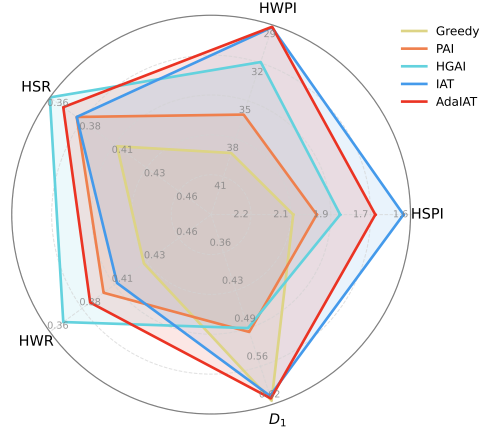


Figure 7. Results of HalluBench in LLaVA-1.5-7B. Five aspects are analyzed: hallucinated sentences per image (HSPI), hallucinated words per image (HWPI), hallucinated sentences ratio (HSR), hallucinated words ratio (HWR), and Distinct-1 ( $D_1$ ). Larger radar area indicates better performance.

lationships, we further tested the performance of different methods on HalluBench [36]. HalluBench selects 200 images from VG [15] and annotates them with detailed object-level description lists. With the assistance of GPT-4, hallucinations in the generated captions are judged sentence by sentence. The experimental results in LLaVA-1.5-7B are shown in Figure 7. It can be observed that AdaIAT significantly outperforms both PAI and HGAI on HWPI and HSPI, achieving improvements of 17% and 26% compared to Greedy. While HGAI slightly surpasses AdaIAT on HSR and HWR, it exhibits a significant decline on the  $D_1$ . Overall, AdaIAT achieves a better balance across all metrics.

Table 3. Evaluation results of the text quality for captions generated by different methods on LLaVA-1.5-7B.

	Greedy	PAI[21]	HGAI[14]	IAT	AdaIAT
$D_1 \uparrow$	0.614	0.498	0.492	0.609	0.610
$B_{self} \downarrow$	0.058	0.242	0.247	0.090	0.071
$B_r \uparrow$	85.29	84.77	84.78	85.20	85.17
$B_d \uparrow$	59.48	56.80	56.61	58.99	58.29

### 4.5. Generated Text Quality Evaluation

To more comprehensively evaluate the quality of captions generated by different methods, we conducted further experiments on the IIW-400 [11] dataset, which contains 400 images annotated with highly detailed and hallucination-free captions. We evaluated them using  $D_1$  and Self-BLEU [39] ( $B_{self}$ ) for language diversity, as well as BertScore[34] for text quality based on the reference captions.  $B_r$  and  $B_d$  denote the BertScore computed using “roberta-large” and “deberta-xlarge-mnli”, respectively. The experimental results are summarized in the Table 3.

As shown in the results, in terms of  $D_1$  and  $B_{self}$ , both IAT and AdaIAT perform comparably to Greedy. In contrast, PAI and HGAI exhibited significant degradation, revealing the severity of their tendency to produce repetitive text, which substantially harms the linguistic diversity of the model. Similarly, on  $B_r$  and  $B_d$ , PAI and HGAI also demonstrated more pronounced decline. Conversely, AdaIAT outperforms HGAI by 0.39 and 1.68 on  $B_r$  and  $B_d$ , respectively, achieving performance similar to Greedy and thus demonstrating well-preserved text quality.

#### 4.6. Ablations Study

In this section, we conduct ablation analyses using LLaVA-1.5-7B (results for additional models are provided in the Appendix) to investigate parameter sensitivity (the amplification factor  $\alpha$  and the trade-off coefficient  $\beta$ ) and the impact of different layer selections.

**Amplification Factor  $\alpha$ .** As shown in Tab. 4, hallucination rates for both IAT and AdaIAT decrease significantly with increasing  $\alpha$ . However, when  $\alpha$  becomes excessively high ( $\alpha \geq 0.8$  for IAT or  $\alpha \geq 6$  for AdaIAT), the F1 score declines markedly, and  $D_1$  also begins to deteriorate. Considering the hallucination rate, predictive capability, and linguistic quality comprehensively, we selected  $\alpha = 0.8$  for IAT and  $\alpha = 6$  for AdaIAT as the optimal values.

Table 4. Performances of IAT and AdaIAT under different amplification factor  $\alpha$ .

		$\alpha$	0.6	0.7	0.8	0.9	1
IAT	$C_S \downarrow$		36.4	35.2	29.8	21.2	13.6
	$C_I \downarrow$		10.3	10.5	9.0	7.0	5.0
	$F1 \uparrow$		78.1	77.4	76.8	73.5	68.4
	$D_1 \uparrow$		0.62	0.61	0.61	0.57	0.52
		$\alpha$	4	5	6	7	8
AdaIAT	$C_S \downarrow$		34.6	33.8	31.4	31.8	29.4
	$C_I \downarrow$		9.5	9.3	8.3	8.5	8.0
	$F1 \uparrow$		78.9	78.5	79.4	78.7	79.2
	$D_1 \uparrow$		0.60	0.60	0.60	0.59	0.59

Table 5. Performances of AdaIAT under different balanced coefficient  $\beta$ .

$\beta$	0.1	0.3	0.5	0.7	1	1.5
$C_S \downarrow$	32.2	32.6	31.4	33.0	32.6	34.4
$C_I \downarrow$	9.2	8.7	8.3	8.7	8.89	9.66
$F1 \uparrow$	79.1	79.0	79.4	78.8	78.5	78.1
$D_1 \uparrow$	0.599	0.600	0.601	0.597	0.599	0.592

**Balanced coefficient  $\beta$ .** We report the performance of AdaIAT across varying  $\beta$  in Tab. 5. Since  $\beta$  controls the threshold for activating IAT, a small  $\beta$  corresponds to weak intervention, resulting in slight and insignificant hallucination mitigation. As  $\beta$  increases from 0.1 to 0.5, the hallucination rate continuously decreases. However, an excessively high  $\beta$  leads to more frequent activation of IAT, causing abnor-

mally high attention to  $T_p$ , thereby disrupting the model’s inherent prediction patterns. For instance, when  $\beta > 0.5$ , both  $C_S$  and  $C_I$  begin to rise, indicating an increase in hallucination rate. Concurrently, F1 score and  $D_1$  also start to decline. Therefore, to appropriately control the time of IAT activation, we set  $\beta = 0.5$ .

Table 6. The impact of different layer schemes on the hallucination mitigation performance of IAT and AdaIAT.

		Layers	0-5	18-31	0-18	5-31	5-18
IAT	$C_S \downarrow$		24.0	26.0	4.0	1.1	29.8
	$C_I \downarrow$		7.1	8.1	3.3	1.8	9.0
	$F1 \uparrow$		75.3	73.8	48.5	30.3	76.8
	$D_1 \uparrow$		0.582	0.604	0.163	0.036	0.606
AdaIAT	$C_S \downarrow$		45.2	43.8	27.4	29.0	31.4
	$C_I \downarrow$		12.9	11.9	7.1	8.6	8.3
	$F1 \uparrow$		77.3	78.5	77.2	78.4	79.4
	$D_1 \uparrow$		0.583	0.612	0.537	0.616	0.601

**Selection of the Layers to Intervene.** To further investigate the impact of intervening at the shallow (0–5), intermediate (5–18), and deep(18–31) layers, we designed five different layer selection schemes and report the experimental results in Tab. 6. For AdaIAT, intervening solely in shallow or deep layers yielded only marginal hallucination mitigation. Combining intermediate with shallow layers severely degraded textual diversity, whereas adding deep layers led to decreased model accuracy, as reflected in a lower F1 score. In contrast, IAT applied only to shallow or deep layers more aggressively reduced hallucinations but at the expense of prediction richness and accuracy (manifested by a reduced F1 score), with the former also sacrificing some textual diversity ( $D_1$  dropped by approximately 0.02); combining intermediate with shallow or deep layers caused model collapse. Therefore, we chose the more balanced-performing intermediate layers for intervention.

## 5. Conclusion

In this work, to address the concern that existing attention intervention methods induce repetitive descriptions, we first analyze attention patterns during real and hallucinated object token generations, revealing that the generated text tokens facilitate real object prediction. Building on this insight, we propose *Increased Attention to Generated Text* (IAT), thereby significantly reducing the hallucination rate while effectively preserving the model’s inherent linguistic capability. To further maintain prediction capability, we propose *Adaptive IAT* (AdaIAT), which employs a layer-wise adaptive threshold controlling intervention time and fine-grained amplification magnitudes tailored to each attention head’s characteristics. Both analysis and experiments demonstrate that the proposed AdaIAT can achieve a good trade-off between hallucination rate, prediction capability, and textual diversity.

## References

- [1] J.-B. Alayrac, J. Donahue, P. Luc, et al. Flamingo: a visual language model for few-shot learning. In *Proceedings of the Advances in neural information processing systems*, 35:23716–23736, 2022. 2
- [2] W. An, F. Tian, S. Leng, et al. Mitigating object hallucinations in large vision-language models with assembly of global and local attention. In *Proceedings of the Computer Vision and Pattern Recognition Conference*, pages 29915–29926, 2025. 2
- [3] J. Bai, S. Bai, S. Yang, et al. Qwen-vl: A versatile vision-language model for understanding, localization, text reading, and beyond. *arXiv preprint arXiv:2308.12966*, 2023. 1, 6
- [4] S. Bai, K. Chen, X. Liu, et al. Qwen2. 5-vl technical report. *arXiv preprint arXiv:2502.13923*, 2025. 2
- [5] Z. Bai, P. Wang, T. Xiao, et al. Hallucination of multimodal large language models: A survey. *arXiv preprint arXiv:2404.18930*, 2024. 1
- [6] A. Ben-Kish, M. Yanuka, M. Alper, et al. Mitigating open-vocabulary caption hallucinations. In *Proceedings of the 2024 Conference on Empirical Methods in Natural Language Processing*, pages 22680–22698, 2024. 7
- [7] T. Brown, B. Mann, N. Ryder, et al. Language models are few-shot learners. In *Proceedings of the Advances in neural information processing systems*, 33:1877–1901, 2020. 2
- [8] K. Chen, Z. Zhang, W. Zeng, et al. Shikra: Unleashing multimodal llm’s referential dialogue magic. *arXiv preprint arXiv:2306.15195*, 2023. 1
- [9] X. Chen, Z. Wu, X. Liu, et al. Janus-pro: Unified multimodal understanding and generation with data and model scaling. *arXiv preprint arXiv:2501.17811*, 2025. 2, 6
- [10] H. Fang, C. Zhou, J. Kong, et al. Grounding language with vision: A conditional mutual information calibrated decoding strategy for reducing hallucinations in vlms. In *The Thirty-ninth Annual Conference on Neural Information Processing Systems*. 2
- [11] R. Garg, A. Burns, B. K. Ayan, et al. Imageinwords: Unlocking hyper-detailed image descriptions. In *Proceedings of the 2024 Conference on Empirical Methods in Natural Language Processing*, pages 93–127, 2024. 7
- [12] A. Gunjal, J. Yin, and E. Bas. Detecting and preventing hallucinations in large vision language models. In *Proceedings of the AAAI Conference on Artificial Intelligence*, pages 18135–18143, 2024. 2
- [13] C. Jiang, H. Xu, M. Dong, et al. Hallucination augmented contrastive learning for multimodal large language model. In *Proceedings of the IEEE/CVF Conference on Computer Vision and Pattern Recognition*, pages 27036–27046, 2024. 4
- [14] Z. Jiang, J. Chen, B. Zhu, et al. Devils in middle layers of large vision-language models: Interpreting, detecting and mitigating object hallucinations via attention lens. In *Proceedings of the Computer Vision and Pattern Recognition Conference*, pages 25004–25014, 2025. 1, 2, 3, 6, 7
- [15] R. Krishna, Y. Zhu, O. Groth, et al. Visual genome: Connecting language and vision using crowdsourced dense image annotations. *International journal of computer vision*, 123(1):32–73, 2017. 7
- [16] S. Leng, H. Zhang, G. Chen, et al. Mitigating object hallucinations in large vision-language models through visual contrastive decoding. In *Proceedings of the IEEE/CVF Conference on Computer Vision and Pattern Recognition*, pages 13872–13882, 2024. 2
- [17] J. Li, M. Galley, C. Brockett, et al. A diversity-promoting objective function for neural conversation models. In *Proceedings of the 2016 Conference of the North American Chapter of the Association for Computational Linguistics: Human Language Technologies*, pages 110–119, San Diego, California, 2016. Association for Computational Linguistics. 4
- [18] J. Li, D. Li, S. Savarese, et al. Blip-2: Bootstrapping language-image pre-training with frozen image encoders and large language models. In *Proceedings of the International conference on machine learning*, pages 19730–19742. PMLR, 2023. 2
- [19] T. Lin, M. Maire, S. Belongie, et al. Microsoft coco: Common objects in context. In *Proceedings of the European conference on computer vision*, pages 740–755. Springer, 2014. 3, 4
- [20] H. Liu, C. Li, Y. Li, et al. Improved baselines with visual instruction tuning. In *Proceedings of the IEEE/CVF Conference on Computer Vision and Pattern Recognition*, pages 26296–26306, 2024. 2, 6
- [21] S. Liu, K. Zheng, and W. Chen. Paying more attention to image: A training-free method for alleviating hallucination in vlms. In *Proceedings of the European Conference on Computer Vision*, pages 125–140. Springer, 2024. 1, 2, 6, 7
- [22] B. Peng, C. Li, P. He, et al. Instruction tuning with gpt-4. *arXiv preprint arXiv:2304.03277*, 2023. 2
- [23] A. Radford, J. W. Kim, C. Hallacy, et al. Learning transferable visual models from natural language supervision. In *Proceedings of the International conference on machine learning*, pages 8748–8763. PMLR, 2021. 2
- [24] A. Rohrbach, L. A. Hendricks, K. Burns, et al. Object hallucination in image captioning. In *Proceedings of the 2018 Conference on Empirical Methods in Natural Language Processing*, pages 4035–4045, 2018. 4
- [25] Z. Sun, S. Shen, S. Cao, et al. Aligning large multimodal models with factually augmented rlhf. *arXiv preprint arXiv:2309.14525*, 2023. 2
- [26] F. Tang, Z. Huang, C. Liu, et al. Intervening anchor token: Decoding strategy in alleviating hallucinations for mllms. In *The Thirteenth International Conference on Learning Representations*, 2025. 2
- [27] S. Tong, Z. Liu, Y. Zhai, et al. Eyes wide shut? exploring the visual shortcomings of multimodal llms. In *Proceedings of the IEEE/CVF Conference on Computer Vision and Pattern Recognition*, pages 9568–9578, 2024. 1
- [28] H. Touvron, T. Lavril, G. Izacard, et al. Llama: Open and efficient foundation language models. *arXiv preprint arXiv:2302.13971*, 2023. 2
- [29] C. Wang, X. Chen, N. Zhang, et al. Mllm can see? dynamic correction decoding for hallucination mitigation. In *The Thirteenth International Conference on Learning Representations*. 1

- [30] J. Wei, M. Bosma, V. Y. Zhao, et al. Finetuned language models are zero-shot learners. *arXiv preprint arXiv:2109.01652*, 2021. [2](#)
- [31] T. Yang, Z. Li, J. Cao, et al. Understanding and mitigating hallucination in large vision-language models via modular attribution and intervention. In *The Thirteenth International Conference on Learning Representations*, 2025. [2](#)
- [32] S. Yin, C. Fu, S. Zhao, et al. Woodpecker: Hallucination correction for multimodal large language models. *Science China Information Sciences*, 67(12):220105, 2024. [2](#)
- [33] Q. Yu, J. Li, L. Wei, et al. Hallucidoctor: Mitigating hallucinatory toxicity in visual instruction data. In *Proceedings of the IEEE/CVF Conference on Computer Vision and Pattern Recognition*, pages 12944–12953, 2024. [4](#)
- [34] T. Zhang, V. Kishore, F. Wu, et al. Bertscore: Evaluating text generation with bert. In *Proceedings of the International Conference on Learning Representations*, 2020. [7](#)
- [35] X. Zhang, Y. Quan, C. Gu, et al. Seeing clearly by layer two: Enhancing attention heads to alleviate hallucination in vlms. *arXiv preprint arXiv:2411.09968*, 2024. [2](#)
- [36] Z. Zhao, B. Wang, L. Ouyang, et al. Beyond hallucinations: Enhancing vlms through hallucination-aware direct preference optimization. *arXiv preprint arXiv:2311.16839*, 2023. [7](#)
- [37] Y. Zhou, C. Cui, J. Yoon, et al. Analyzing and mitigating object hallucination in large vision-language models. In *Proceedings of the The Twelfth International Conference on Learning Representations*, 2024. [2](#)
- [38] D. Zhu, J. Chen, X. Shen, et al. Minigpt-4: Enhancing vision-language understanding with advanced large language models. *arXiv preprint arXiv:2304.10592*, 2023. [1](#)
- [39] Y. Zhu, S. Lu, L. Zheng, et al. Taxygen: A benchmarking platform for text generation models. In *Proceedings of the The 41st international ACM SIGIR conference on research & development in information retrieval*, pages 1097–1100, 2018. [7](#)
- [40] X. Zou, Y. Wang, Y. Yan, et al. Look twice before you answer: Memory-space visual retracing for hallucination mitigation in multimodal large language models. In *International Conference on Machine Learning*, pages 80873–80899. PMLR, 2025. [2](#)